Front. Earth Sci. 2019, 13(2): 410–421
https://doi.org/10.1007/s11707-018-0732-x

RESEARCH ARTICLE

Terrain relief periods of loess landforms based on terrain profiles of the Loess Plateau in northern Shaanxi Province, China

Jianjun CAO[1,2], Guoan TANG[1], Xuan FANG (✉)[1,2], Jilong LI[1], Yongjuan LIU[2], Yiting ZHANG[2], Ying ZHU[2], Fayuan LI (✉)[1]

1 Key Laboratory of Virtual Geographic Environment of Ministry of Education, Nanjing Normal University, Nanjing 210023, China
2 School of Environment Science, Nanjing Xiaozhuang University, Nanjing 211171, China

Abstract The Loess Plateau is densely covered by numerous types of gullies which represent different soil erosion intensities. Therefore, research on topographic variation features of the loess gullies is of great significance to environmental protection and ecological management. Using a 5 m digital elevation model and data from a national geographic database, this paper studies different topographical areas of the Loess Plateau, including Shenmu, Suide, Yanchuan, Ganquan, Yijun, and Chunhua, to derive representative gully terrain profile data of the sampled areas. First, the profile data are standardized in MATLAB and then decomposed using the ensemble empirical mode decomposition method. Then, a significance test is performed on the results; the test confidence is 95% to 99%. The most reliable decomposition component is then used to calculate the relief period and size of the gullies. The results showed that relief periods of the Chunhua, Shenmu, Yijun, Yuanchuan, Ganquan, and Suide gullies are 1110.14 m, 1096.85 m, 1002.49 m, 523.48 m, 498.12 m, and 270.83 m, respectively. In terms of gully size, the loess landforms are sorted as loess fragmented tableland, aeolian and dune, loess tableland, loess ridge, loess hill and loess ridge, and loess hill, in descending order. Taken together, the gully terrain features of the sample areas and the results of the study are approximately consistent with the actual terrain profiles. Thus, we conclude that ensemble empirical mode decomposition is a reliable method for the study of the relief and topography of loess gullies.

Keywords loess gully, DEM, terrain profile, EEMD, Loess Plateau

Received January 10, 2018; accepted August 14, 2018

E-mails: fangxuan1982@163.com (Xuan FANG);
lifayuan@njnu.edu.cn (Fayuan LI)

1 Introduction

The Loess Plateau contains the world's largest distribution of loess soils (Liu et al., 1991) and also suffers from some of the worst cases of soil erosion globally (Cai, 2001). Soil erosion leads to damaged soil resources, degradation of soil fertility and quality, worsening ecological environments, infrastructure destruction (Blanco and Lal, 2010; Zhao et al., 2013; Xu et al., 2016; Fu et al., 2017), and flooding events (Zhang et al., 2016a, b). Therefore, soil erosion is a major environmental issue for the survival and development of mankind. The unique crisscrossing gullies of the Loess Plateau were formed by long periods of severe soil erosion (Vandaele et al., 1996; Valentin et al., 2005; Cheng et al., 2007; Svoray and Markovitch, 2009; Zhu, 2012; Sun et al., 2014; Torri and Poesen, 2014; Li et al., 2015), and the topographic features of these eroded gullies also have important impacts on soil erosion (Li et al., 2016). Therefore, studying the topographic features and spatial distribution of gullies is extremely significant for water and soil resource conservation in the Loess Plateau as well as for the rehabilitation of its ecosystems.

Early studies on gullies in the Loess Plateau were characterized by qualitative research. The earliest and most representative study is on loess gully classification, which is based on the landform scale and soil erosion type of loess gullies (Luo, 1956; Zhu, 1956). Further research on loess gully classification considered variations in gully development position, morphological features, and soil erosion (Chen, 1984; Liu et al., 1988; Tang et al., 1998). Lei et al. (2000) put forward the concept of soil erosion chains through the evolution of soil erosion processes and used system dynamics to link the erosion gully network of the Loess Plateau. This above-mentioned research enriched the loess gully geomorphology and soil science

and laid a theoretical foundation for the quantitative research in loess gully terrain.

The topographic features of gullies have been studied since the 1940s. In 1945, Horton (1945) proposed four metric laws for flow lengths and drainage areas, which eventually became known worldwide as "Horton's Laws." The laws have had a profound impact on the quantitative study of gully topography. At present, profile analysis is the most commonly used method for studying topographic features quantitatively (Hack, 1973; Avouac et al., 1996; Telbisz et al., 2013; Jiang et al., 2016; Ma et al., 2017). Topographic profile analysis utilizes a digital elevation model (DEM) as a basis for creating profiles in a given direction, and then employs profile data to express the topographic and hydrologic features of a study area. Burbank (1992) extracted elevation data corresponding to the uplift and denudation processes of the Qinghai-Tibet Plateau, analyzing the relationship between these processes and the distribution of slope gradients. Fielding et al. (1994) calculated the maximum, minimum, and average elevation profiles of the Qinghai-Tibet Plateau and generated sampling profiles of the plateau. The profile data were then combined with slope surface analysis; it was concluded that the Qinghai-Tibet Plateau has characteristically mild slope distributions, especially in the northern and central areas. Zhao et al. (2009) employed linear and swath topographic profiles to study the relationship between topographic gradient and the uplift process of Kongur Tagh, a mountain which is located in the northern Qinghai-Tibet Plateau. The linear topographic profiles produced were direct and clear, and the generated swath profiles were an excellent reflection of the region's topographic relief. Based on the Shuttle Radar Topography Mission (SRTM) DEM of the United States and 1:5,000,000 digital geologic maps, Cheng et al. (2007) utilized topography elevation profile analysis methods to conclude that rift gullies, fault-block mountains, and rift basins coexist in the Dabie Mountains. Furthermore, statistical methods were employed to obtain the swath profiles and the maximum, minimum, and average elevation values of the Dabie Mountains. Results showed that the slope, topographic relief, and average elevation in the same areas are interrelated, and the geomorphic features of the Dabie Mountains were thus revealed by this study. Zhang et al. (2006a,b) used SRTM data to obtain the topographic relief of the Loess Plateau via elevation profiles and thresholds. Having extended the technical methods available for the acquisition of topographic relief, they then performed a preliminary quantitative study on erosion in the Loess Plateau. Zou et al. (2011) extracted swath profiles and formed a complete set of technical procedures. The swath profiles were employed to quantitatively analyze the geomorphic features of the Three Gorges region. These studies demonstrated that profile analysis is an effective method for analyzing a region's geography quantitatively.

Since the 1970s, spatial frequency spectrum analysis methods, such as Fourier transformations and wavelet decomposition, have been broadly applied to topographic analyses (Rayner, 1972; Pike and Rozema, 1975). Hanley (1977) used 2D Fourier transforms to simulate the hillocks of the Catawba Mountains in Virginia, USA. Harrison and Lo (1996) utilized 2D fast Fourier transformations to simulate the karst areas of Puerto Rico, concluding that Fourier analysis can be used for topographic reconstructions. Yu et al. (2004) applied wavelet decomposition to describe the assignment of contour lines in 3D topography models. When Perron et al. (2008) employed 2D Fourier frequency spectrum to investigate the topography of northern California, they concluded that a correspondence exists between the frequency obtained with Fourier analysis and slope length. Simultaneously, scholars have also conducted extensive investigations in topographic analysis using spatial frequency spectrums. Based on theories of wavelet multi-resolution analysis, Wu (2003) utilized the norm of wavelet coefficients as a quantitative index for generalizing a corresponding scale. Previous research (Li, 2008; Chen et al., 2012) employed wavelet fractal analysis to construct multi-scale DEM models and multi-scale DEM representations. Other research (Li et al., 2007; Chen and Zhou, 2013) combined wavelet multi-scale analysis with square root models to synthesize DEM data. Utilizing Fourier transformations and spectral analysis, later research (Frederiksen, 1981; Doglioni and Simeone, 2014; Davis and Chojnacki, 2017) analyzed the features and range of erosion-related topographic features in the extracted topographic profiles of erosion gully areas in the Loess Plateau, and the low, moderate, and high frequency of topographic features were successfully separated.

The ensemble empirical mode decomposition (EEMD) method is effective for spatial spectrum analysis. Cao et al. (2017) employed EEMD and multifractal detrended fluctuation analysis (MF-DFA) to characterize the embedded noise in topographic profiles of shoulder lines, developing the methods for extracting and removing this noise. The EEMD method, without the need for human set decomposition conditions, can obtain loess gully terrain frequency, relief period, and the size distribution characteristics of different landform types in the Loess Plateau gullies and ravines. Very little literature exists on the spatial distribution frequency of loess gullies in different landforms. Therefore, taking the Shenmu, Suide, Yanchuan, Ganquan, Yijun, and Chunhua area of the Loess Plateau as sampling areas, representative topographic profiles were extracted from a 1:10000 DEM of the study areas. EEMD was then performed on these profiles after standardization, and significance tests were conducted. The spatial features and distribution frequency of topographic variations in the six sampling areas were obtained from analyzing the intrinsic mode functions (IMFs), with high levels of significance. Finally, the spatial

distribution patterns of gullies with different scales were determined.

2 Materials and methods

2.1 Study area and research data

The study area comprised the Shenmu, Suide, Yanchuan, Ganquan, Yijun, and Chunhua sample areas (Fig. 1 and Table 1); these six areas are located from the northern to the southern regions of the Loess Plateau, successively. The DEMs used in this study were from the National Administration of Surveying, Mapping, and Geoinformation of China and were generated by 1: 10000 topographic maps with a 1 m contour interval. First, the paper topographic maps were drawn by the ground-based surveys and then scanned into the computer with a geometric correction. Then, the contour lines were digitalized and interpolated into a triangulated irregular network (TIN). Finally, the gridded DEMs were interpolated by the TIN after ordinary manual editing in TIN to correct mistakes. Representative profile data were extracted from the six watersheds. Starting with the gully openings, elevation data were sampled from the gullies' negative relief regions using the DEMs. Thus, the 2D data corresponding to the change in elevation with distance, i.e., the topographic profiles (Figs. 2(a)–2(f)), were obtained.

2.2 Methods

As conventional Fourier transformations and wavelet decomposition are based on pre-determined basis functions, these methods are not data-adaptive and may generate spurious decomposed fluctuation scales (Alexandrov, 2009; Ayenu-Prah and Attoh-Okine, 2009). Compared to these methods, the greatest strength of empirical mode decomposition (EMD) (Huang et al., 1998), a signal analysis method, is that it is data-adaptive, and thus can decompose any type of signal. EMD is also suitable for nonstationary and nonlinear data and is broadly applied to these types of signal sequences.

The objective of EMD is to decompose raw signals that are difficult to analyze into a set of highly analyzable IMFs to elucidate signal features. The generated IMFs must have physical significance in order to produce an accurate decomposition representation of a signal's variation characteristics. Therefore, an IMF needs to satisfy the following requirements. First, the number of extrema in the entirety of the signal data must be exactly equal to the number of zero crossings. Second, at any distance point, the upper envelope formed by local maxima and the lower envelope formed by local minima must have an average value of zero.

Although EMD is an adaptive method, it still suffers from certain flaws, such as endpoint effects and scale mixing from the influence of the original signal frequencies. To address these issues, Wu and Huang (2009) proposed a type of noise-assisted data analysis based on the EEMD method, which overcomes the mode mixing issues of EMD by screening IMF components with added white noise. Moreover, the perturbations of the ensemble white noise provide a mechanism for significance tests within the EEMD method to obtain confidence levels for

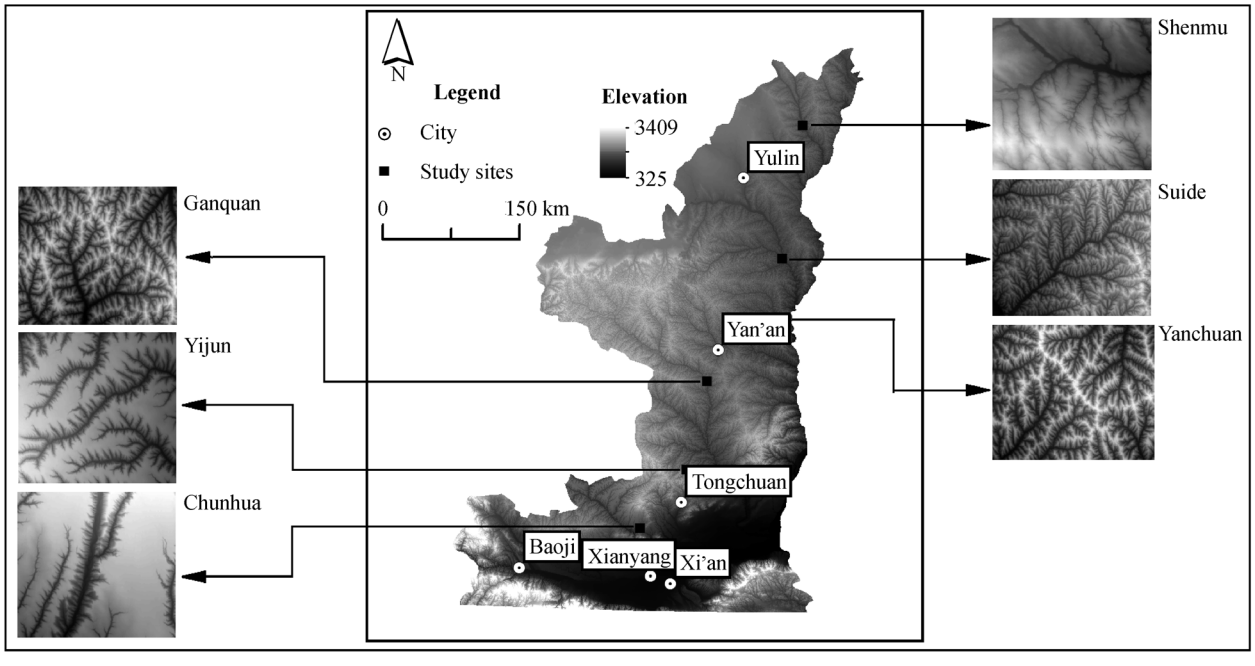

Fig. 1 The study area and sampling sites.

Table 1 Geographic description of the study sites

Sampling sites	Geographic location	Landform types	Location description
Shenmu	109°40′00″–110°54′00″E 38°50′00″–38°55′00″N	Aeolian and dune	In Shenmu sample area, elevation is 1060–1322 m, with an average slope of 9° and gully density of 3.4 km/km^2. Contiguous low hills covered by thin layers of sand and gently inclined dunes are found throughout this region
Suide	110°15′00″–110°22′30″E 37°32′30″–37°37′30″N	Loess hill	In Suide sample area, elevation is 847–1163 m, with an average slope of 29° and gully density of 6.52 km/km^2. The area is hilly and crisscrossed with gullies, with extremely severe soil erosion
Yanchuan	109°52′30″–110°00′00″E 36°42′30″–36°47′30″N	Loess ridge-hill	In Yanchuan sample area, elevation is 953–1252 m, with an average slope of 31° and gully density of 6.78 km/km^2. Rills and ephemeral gullies have developed on the ridges, and gulches, ditches, and streams have incised deeply below the loess ridges and hills
Ganquan	109°30′00″–109°37′30″E 36°10′00″–36°15′00″N	Loess ridge	In Ganquan sample area, elevation is 1149–1445 m, with an average slope of 27° and gully density of 5.6 km/km^2. Ridge slopes are eroded, and intense down-incising gulches and streams occur between ridges
Yijun	109°18′45″–109°26′15″E 35°25′00″–35°30′00″N	Loess tableland	In Yijun sample area, elevation is 797–1134 m, with an average slope of 19° and gully density of 4.2 km/km^2. Headward gully erosion is extremely severe, and gravitational erosion is active in this area
Chunhua	108°22′30″–108°30′00″E 34°50′00″–34°55′00″N	Loess fragmented tableland	In Chunhua sample area, elevation is 768–1164 m, with an average slope of 12° and gully density of 3.13 km/km^2. The loess tableland and residual tableland are the primary landforms of this area, but these have been deeply incised by a number of large gullies

each IMF, which was previously impossible with the EMD method (Wu and Huang, 2004, 2005).

The operational procedures of the EEMD method are as follows:

1) A white noise sequence, $w(t)$, is added to an original data sequence, $x(t)$, at a certain signal-to-noise ratio (SNR), which yields an overall signal:

$$X(t) = x(t) + w(t). \tag{1}$$

2) EMD decomposition is performed on the new data sequence, i.e., the data sequence that has been superimposed with white noise, to obtain each IMF component:

$$X(t) = \sum_{i=1}^{n} c_i + r_n. \tag{2}$$

3) The aforementioned procedures are repeated, and a new generated white noise sequence $w(t)$ with the same amplitude is added to the original signal in each repetition:

$$X_j(t) = \sum_{i=1}^{n} c_{ji} + r_{jn}. \tag{3}$$

4) The corresponding IMF component, $c_n(t)$, of each original signal is expressed as:

$$c_n(t) = \frac{1}{N}\sum_{j=1}^{N} c_{j,n}(t). \tag{4}$$

5) The final result of the decomposition is:

$$x(t) = \sum_{n=1}^{m} c_n(t) + r_m(t). \tag{5}$$

Significance tests may then be performed to determine whether the IMF components obtained from the decomposition are physically significant or mere noise. The properties of each IMF component may be determined by analyzing the distribution of their energy spectral density periods, from which the required IMF components are selected for analysis. The energy spectral density of the k^{th} IMF component is:

$$E_k = \frac{1}{n}\sum_{j=1}^{N} |I_k(j)|^2. \tag{6}$$

In this equation, N represents the length of the IMF component while $I_k(j)$ is the k^{th} IMF component. Using the Monte Carlo method to perform a test on the white noise sequence, the approximate relationship between the average energy spectral density value, $\overline{E}_k$, and average period, $\overline{T}_k$, of the k^{th} IMF component may be expressed as:

$$\ln\overline{E}_k + \ln\left\{\overline{T}_K\right\}_a = 0. \tag{7}$$

By mapping $\ln\left\{\overline{T}_K\right\}_a$ as the horizontal x-axis and $\ln\overline{E}_k$ as the vertical y-axis, the relationship between these two variables will be displayed as a straight line with a slope of –1. In theory, the constant IMF component of the white noise should lie on this straight line, but deviations will occur to some extent in practice. Therefore, the confidence interval of the white noise's energy spectral distribution is:

$$\ln\overline{E}_k = \ln\{\overline{T}_K\}_a \pm \alpha\sqrt{\frac{2}{Ne}}^{\ln\left(\frac{\{\overline{T}_K\}_a}{2}\right)}, \qquad (8)$$

where α is the significance level.

In this study, the EEMD method was employed to standardize and decompose the profile elevation data extracted from six sample areas in the Loess Plateau, i.e., Shenmu, Suide, Yanchuan, Ganquan, Yijun, and Chunhua, thereby obtaining the decomposed components of the profile elevation signals. Significance tests were implemented on the results of the decomposition, and IMFs with the highest confidence levels were selected. The periods and frequencies of these IMFs were calculated and combined with topographic knowledge. Then, the spatial characteristics and distribution frequencies of the topographic variation of gullies in different landforms were subsequently obtained. After the comparison among different landforms, we acquired the spatial distribution patterns of the gullies.

3 Results and discussion

3.1 Gully profile decomposition and tests

Due to the self-adaptation of the EEMD decomposition method, the decomposition results of each study area completely depend on the profile data. The decomposition results of Shenmu, Suide, and Yijun sampling areas have 10 IMF components and a residual trend value (RES) (Figs. 3, 4, and 7), while the decomposition results of Yanchuan, Ganquan, and Chunhua areas comprise 9 IMF components and an RES value (Figs. 5, 6, and 8).

In the six different geomorphological study area types including tablelands, ridges and hills, various types of gullies with different scales, gully densities, and incision depths are formed due to the variations of underlying bedrock, rainfall, and soil erosion. The period and frequencies of the topographic relief of gullies in different landforms are diverse because of the nesting of different levels of gullies in the watershed. The period and frequency of the topographic relief of gullies in the same landform are also different. The IMF components of the decomposition results of the gully topographic profiles reflect the fluctuation characteristics of topographic relief from high frequency to low frequency. Each of the IMF components decomposed by EEMD is independently representative, i.e., there are no oscillations with the same period and frequency of terrain relief in each study area. Moreover, each IMF component is characteristic of a physical feature, respectively revealing the terrain oscillations of different characteristic scales inherent in the original terrain profile. This non-uniform variation in the topographic intensity of the terrain embodies the nonlinear interaction between the dynamic process and the external

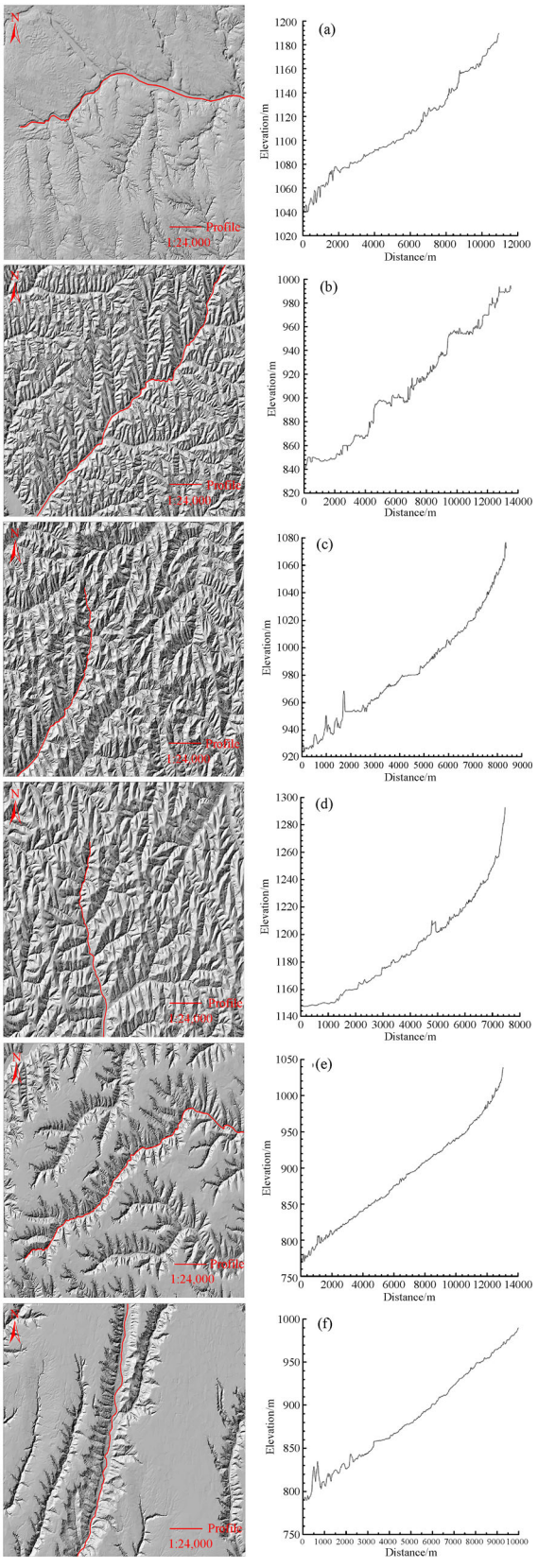

Fig. 2 The six types of loess landform and the profile of gully, (a) Shenmu; (b) Suide; (c) Yanchuan; (d) Ganquan; (e) Yijun; (f) Chunhua.

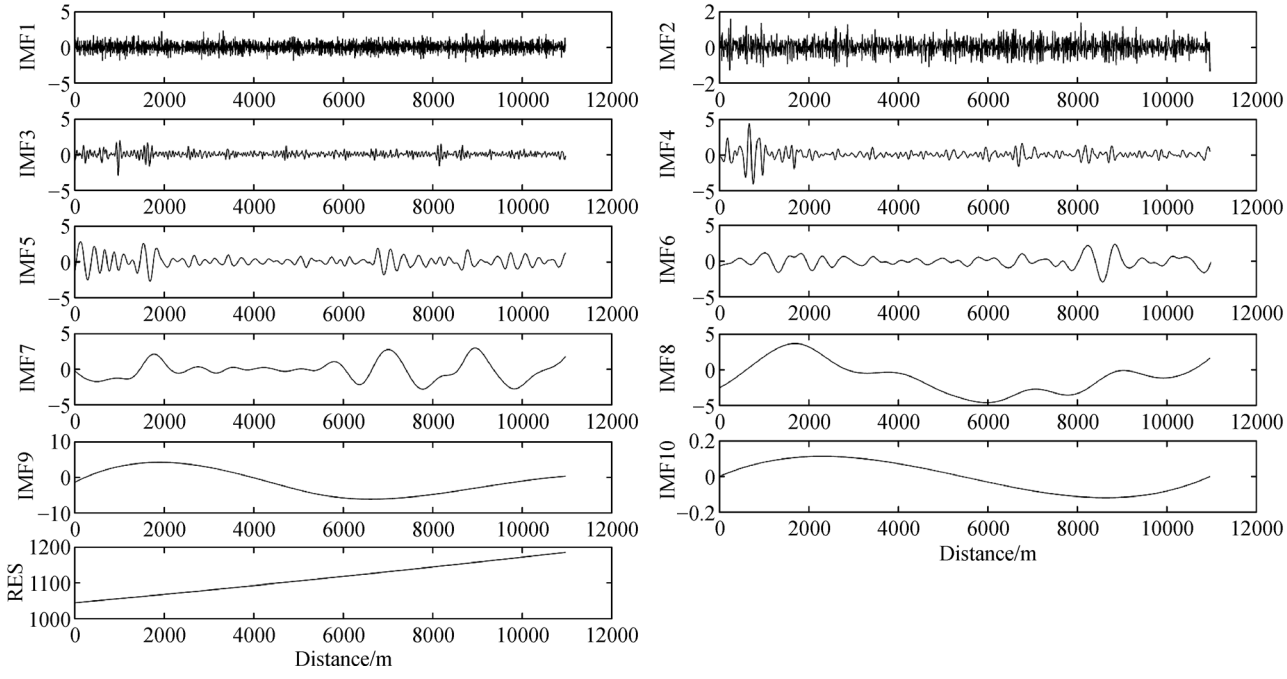

Fig. 3 The decomposition by EEMD of gully topographic in Shenmu site.

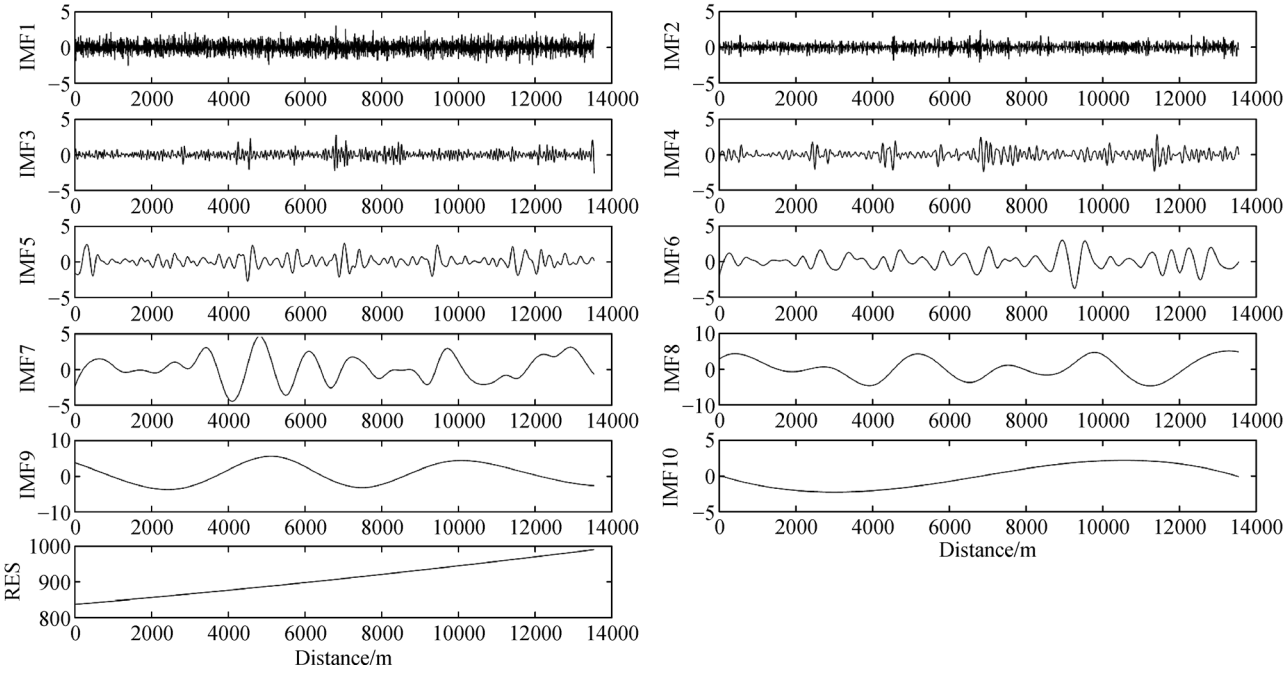

Fig. 4 The decomposition by EEMD of gully topographic in Suide site.

factors of the topography of the Loess Plateau. In order to analyze the different characteristic scale oscillations inherent in the topographic relief of different landform types, the mean period of topographic relief was calculated. Furthermore, the degree of influence of the frequency and amplitude of the IMF fluctuations at each scale on the overall characteristics of the original terrain profile data are represented by the variance contribution rate, as shown in Table 2. For the sake of testing whether the decomposed IMF components are pure noise or components with physical meaning in the original gully terrain profiles, significance tests were employed.

Table 2 displays the average period of different terrain relief and variance contribution rates of each IMF

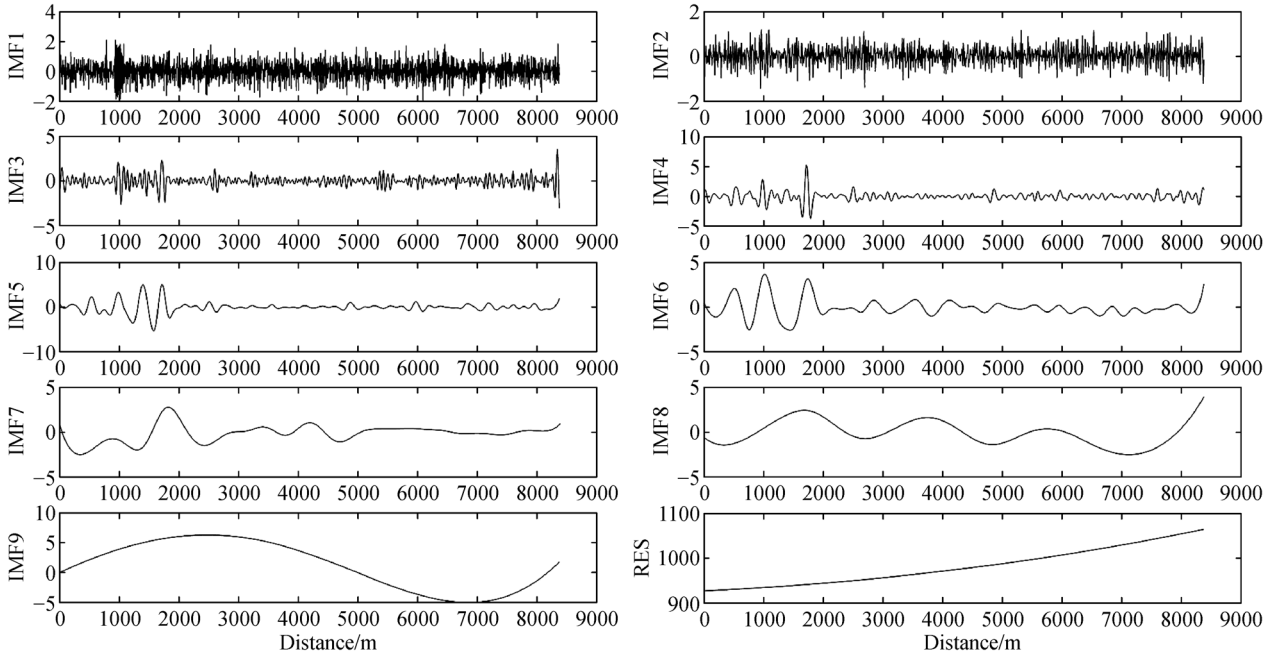

Fig. 5 The decomposition by EEMD of gully topographic in Yanchuan site.

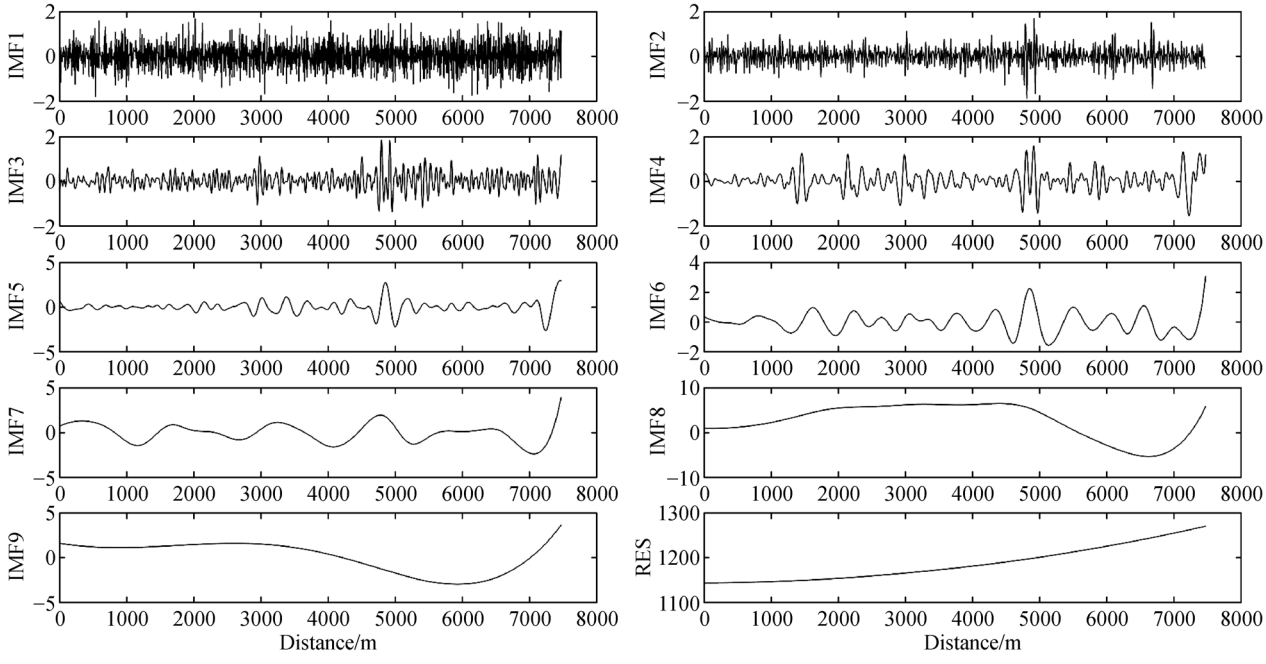

Fig. 6 The decomposition by EEMD of gully topographic in Ganquan site.

component represented by different scales. Significance levels α were selected as 0.01 and 0.05, respectively (Table 2 and Figs. 9(a)–9(f). An IMF located above the confidence curve indicates that it has passed the significance test and therefore contains information with actual physical meaning within the selected confidence level. Conversely, if the energy of the decomposed IMF lies below the confidence curve with respect to the period distribution, it has failed the significance test, indicating that the information contained in the IMF consists of mainly white noise components. In Figs. 9(a)–9(f), the closer to the left the IMF component is, the higher the terrain relief frequency and the smaller the relief period will be. The vertical axis represents the Energy Spectral

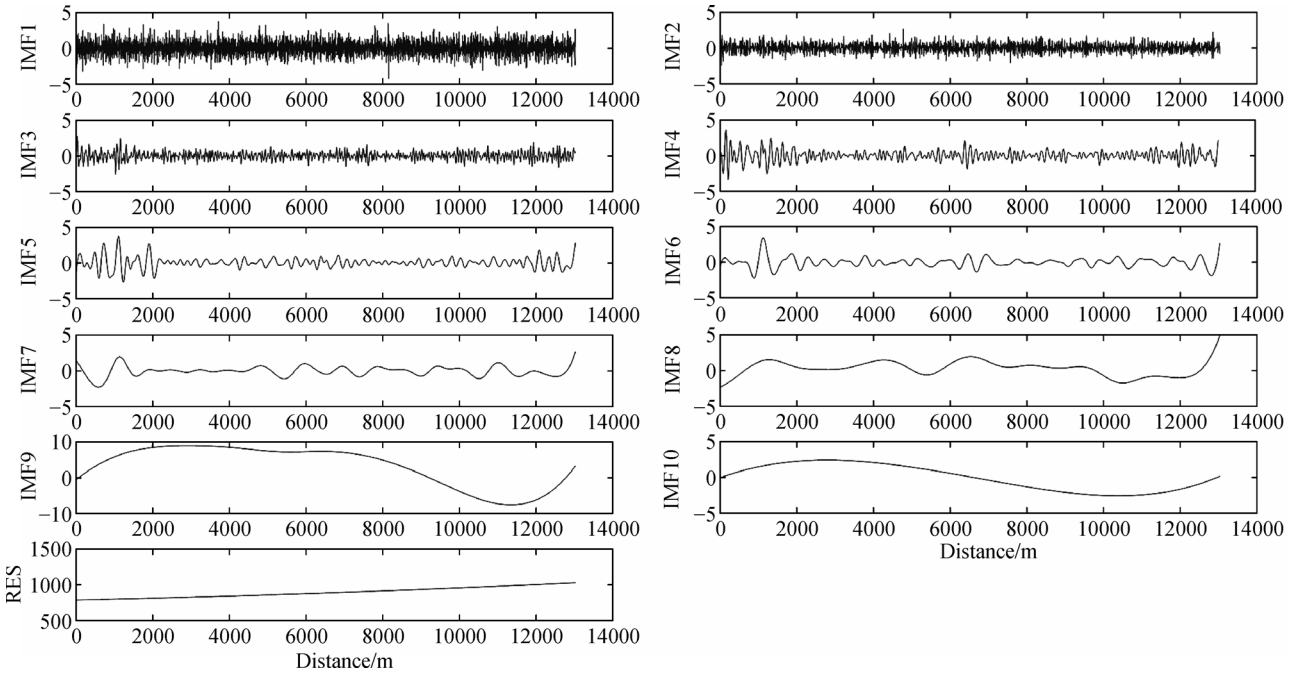

Fig. 7 The decomposition by EEMD of gully topographic in Yijun site.

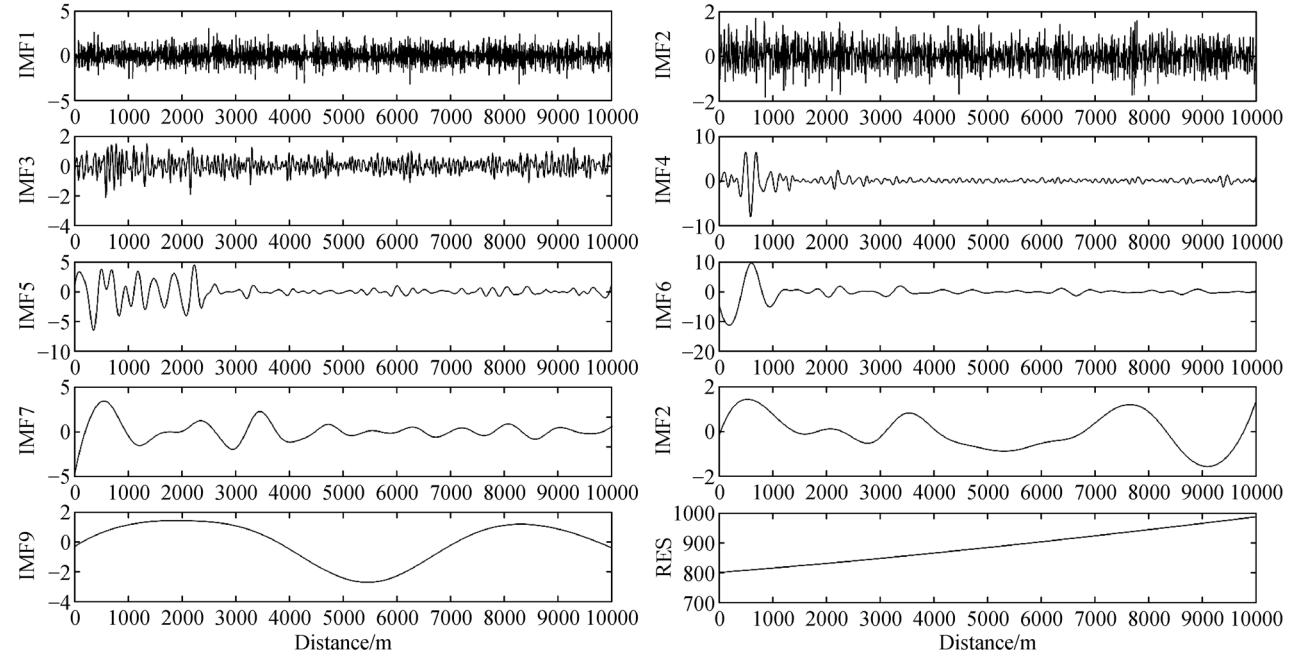

Fig. 8 The decomposition by EEMD of gully topographic in Chunhua site.

Density (ESD) of the IMF component. The closer to the upper side, the higher the energy that the IMF component has and the larger the amplitude is.

3.2 Topography relief features of gullies

From Fig. 9(a), it can be seen that IMF9 and IMF10 fall below the 95% confidence level, and thus contain relatively little physical information. IMF1 to IMF8 fall above the 99% confidence level and include more physical information. Table 2 also gives the variance contribution rate of each component of EEMD. It should be noted that individual IMFs that lie within the significant range of white noise do not meet the significance test, but do factor

Table 2 The parameters of significance test by Monte Carlo of six study sites in Loess Plateau

Sampling site	Parameters	IMF1	IMF2	IMF3	IMF4	IMF5	IMF6	IMF7	IMF8	IMF9	IMF10	RES
Shenmu	Variance contribution rate%	0.0229	0.0081	0.0087	0.0312	0.0342	0.0299	0.0962	0.3453	0.7733	0.001	98.65
	Relief period/m	3.1673	6.7018	13.863	29.47	57.79	120.27	296.67	1483.3	2225	2225	–
	Confidence level	> 99%	> 99%	> 99%	> 99%	> 99%	> 99%	> 99%	> 99%	< 95%	< 95%	–
Suide	Variance contribution rate%	0.0289	0.0118	0.0116	0.0183	0.0296	0.0509	0.1622	0.4577	0.3758	0.1268	98.73
	Relief period/m	3.2411	6.7226	13.815	29.87	58.168	120.13	325.06	690.75	1105.2	1842	–
	Confidence level	> 99%	> 99%	> 99%	> 99%	> 99%	< 95%	> 99%	> 99%	> 99%	> 99%	–
Yanchuan	Variance contribution rate%	0.0201	0.0091	0.0179	0.0316	0.0842	0.0615	0.0456	1.1462	0.1434	–	98.44
	Relief period/m	3.21	6.8942	14.392	29.776	63.963	115.13	431.75	690.8	1727	–	–
	Confidence level	> 99%	> 99%	> 99%	> 99%	> 99%	> 99%	< 95%	> 99%	> 99%	–	–
Ganquan	Variance contribution rate%	0.0207	0.0091	0.0077	0.0118	0.0329	0.0384	0.8343	0.0747	0.1731	–	98.80
	Relief period/m	3.1089	6.6753	14.212	28.294	57.111	128.5	308.4	1542	1542	–	–
	Confidence level	> 99%	> 99%	> 99%	> 99%	> 99%	> 99%	> 99%	> 99%	> 99%	–	–
Yijun	Variance contribution rate%	0.0214	0.0074	0.0063	0.0085	0.0115	0.0075	0.0099	0.6132	0.0185	0.0641	99.23
	Relief period/m	3.2036	6.5079	13.289	29.092	55.485	109.84	207	768.86	1794	2691	–
	Confidence level	> 99%	> 99%	> 99%	> 99%	> 99%	> 99%	> 99%	> 99%	> 99%	> 99%	–
Chunhua	Variance contribution rate%	0.0248	0.0089	0.0071	0.0466	0.0583	0.1512	0.0406	0.0176	0.0578	–	99.59
	Relief period/m	3.2441	6.3869	13.556	28.629	62.03	124.06	372.18	454.89	1023.5	–	–
	Confidence level	> 99%	> 99%	> 99%	> 99%	> 99%	> 99%	> 99%	< 95%	< 95%	–	–

into the calculation of variance contribution rates in order to maintain the total energy of the signal. In the Shenmu area, the variance contribution rate of IMF8 (0.3453) is the highest among all components that passed the significance test, except for the RES (Fig. 3, Fig. 9(a), and Table 2). Therefore, IMF8 is the dominant period of the topographic relief in Shenmu. By calculating the variation period of the IMF8 component, the average period of terrain relief in Shenmu was found to be 1483.3 m.

In the Suide area, IMF6 did not pass the significance test (Fig. 4, Fig. 9(b), and Table 2). Among all the components that passed the significance test, the variance contribution rate of IMF8 (0.4577) is the highest. IMF8 is the dominant period of topographic relief in Suide, and the average period of gully terrain relief was found to be 690.75 m. In the Yanchuan area, IMF7 did not pass the significance test. Of all the components that passed the significance test, the IMF8 component has the highest contribution to the variance (1.1462). Therefore, the main period of topographic relief is IMF8 in Yanchuan, where the average period was found to be 690.8 m (Fig. 5, Fig. 9(c), and Table 2).

All decomposition components in the Ganqun area were above the 99% confidence level, and thus met the significance test. IMF7 had the highest variance contribution rate (0.8343) and was determined to be the main period of the gully topography in Ganquan, with the average period of the relief being 308.4 m (Fig. 6, Fig. 9(d), and Table 2). Similarly, all decomposition components in Yijun are above the 99% confidence level, passing the significance test. In addition to the RES, IMF8 possesses the largest variance contribution rate (0.6132) (Fig. 7, Fig. 9(e), and Table 2). This illustrates that IMF8 is the main period of gully topography in the Yijun area, with an average period of gully topography relief of 768.86 m (Fig. 7).

In the EEMD decomposition results in the Chunhua area, IMF8 and IMF9 are below the 95% confidence level (Fig. 9(f)). These two components did not pass the significance test, indicating that they contain less information about the significance of the actual gully relief. Comparatively, the rest of the decomposition components are located above the 99% confidence level, revealing that they have passed the significance test and contain more information on the topography of the gully. Among the components that passed the significance test, the variance contribution rate of IMF6 of 0.1512 is the highest (Table 2), confirming that IMF6 is the main period of gully

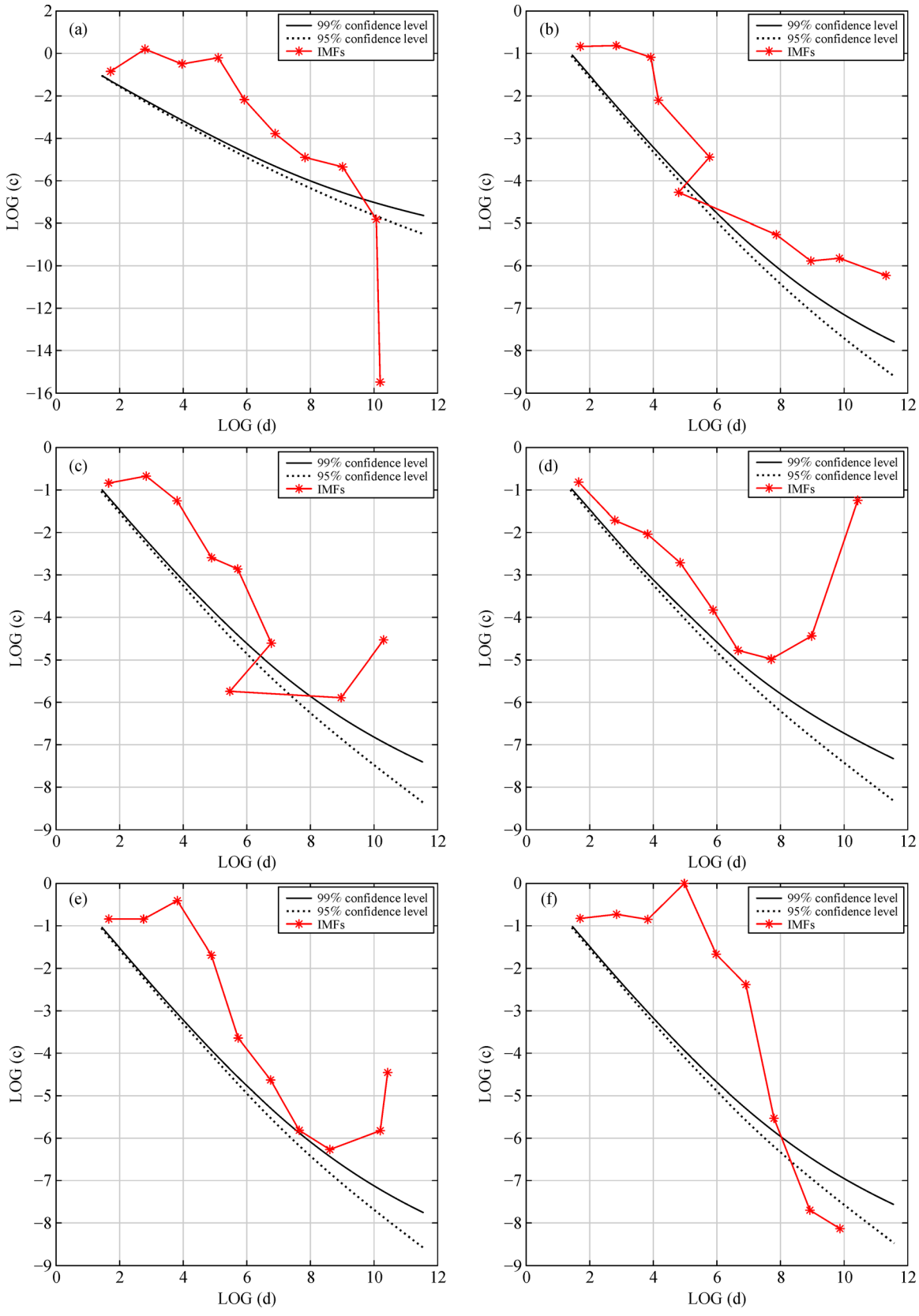

Fig. 9 The significance test by Monte Carlo of gully topographic relief periods in six study sites. (a) Shenmu; (b) Suide; (c) Yanchuan; (d) Ganquan; (e) Yijun; (f) Chunhua.

topography relief in the Chunhua area, with an average period of gully terrain of 124.06 m (Fig. 8).

4 Conclusions

An analysis of gully topographic relief features and spatial distribution frequencies of gullies was proposed based on the decomposition of profile lines. The findings of this study are as follows.

From the EEMD of profile lines, IMFs with high significance accurately reflect the complexity of gully topography. The relief periods of the effective components decreased as gully density increased and vice versa, with a terrain profile order of loess fragmented tableland, aeolian and dune, loess tableland, loess ridge, loess hill and loess ridge, and loess hill gully areas. To conclude, EEMD is an effective method for studying the topographic relief features of loess gullies.

The EEMD decomposition of topographic profiles proposed in this work is a new research methodology for studying topographic relief features of loess gullies. The results of this EEMD-based topographic analysis and topographic scales of gullies were linked based on geomorphic principles, and the spatial distributions of gullies with different scales were compared. However, our understanding of the topographic features of gullies still lacks depth due to the complexity of gully geomorphology and the inherent restrictions of this research method.

Acknowledgements This work was funded by the National Natural Science Foundation of China (Grant Nos. 41471316, 41671389, and 41501487) and the Natural Science Foundation of Jiangsu Province (No. BK20161118). The authors are very grateful to the anonymous referees for their comments provided for improvement of the manuscript.

References

Alexandrov T (2009). A method of trend extraction using singular spectrum analysis. Revstat Stat J, 7(1): 1–22

Avouac J P, Dobremez J F, Bourjot L (1996). Palaeoclimatic interpretation of a topographic profile across middle Holocene regressive shorelines of Longmu Co (western Tibet). Palaeogeogr Palaeoclimatol Palaeoecol, 120(1–2): 93–104

Ayenu-Prah A Y, Attoh-Okine N O (2009). Comparative study of Hilbert–Huang transform, Fourier transform and wavelet transform in pavement profile analysis. VehSystDyn, 47(4): 437–456

Blanco H, Lal R (2010). Principles of Soil Conservation and Management. Springer, 1–19

Burbank D W (1992). Causes of recent Himalayan uplift deduced from deposited patterns in the Ganges basin. Nature, 357(6380): 680–683

Cai Q G (2001). Soil erosion and management on the Loess Plateau. J GeogrSci, 11(1): 53–70

Cao J, Na J, Li J, Tang G, Fang X, Xiong L (2017). Topographic spatial variation analysis of loess shoulder lines in the Loess Plateau of China based on MF-DFA. ISPRS Int J Geoinf, 6(5): 141–159

Chen Y Z (1984). The classification of gully in hilly loess region the middle reaches of the yellow river. Scientia Geographica Sinica, 4(4): 321–327 (in Chinese)

Chen Y, Wilson J P, Zhu Q, Zhou Q (2012). Comparison of drainage-constrained methods for DEM generalization. Comput Geosci, 48: 41–49

Chen Y, Zhou Q (2013). A scale-adaptive DEM for multi-scale terrain analysis. Int J Geogr Inf Sci, 27(7): 1329–1348

Cheng H, Zou X, Wu Y, Zhang C, Zheng Q, Jiang Z (2007). Morphology parameters of ephemeral gully in characteristics hillslopes on the Loess Plateau of China. Soil Tillage Res, 94(1): 4–14

Davis J D, Chojnacki J D (2017). Two-dimensional discrete Fourier transform analysis of karst and coral reef morphologies. Trans GIS, 21(3): 521–545

Doglioni A, Simeone V (2014). Geomorphometric analysis based on discrete wavelet transform. Environ Earth Sci, 71(7): 3095–3108

Fielding E, Isacks B, Barazangi M, Duncan C (1994). How flat is Tibet? Geology, 22(2): 163–167

Frederiksen P (1981). Terrain analysis and accuracy prediction by means of the Fourier transformation. Photogrammetria, 36(4): 145–157

Fu B, Wang S, Liu Y, Liu J, Liang W, Miao C (2017). Hydrogeomorphic ecosystem responses to natural and anthropogenic changes in the Loess Plateau of China. Annu Rev Earth Planet Sci, 45(1): 223–243

Hack J T (1973). Stream-profile analysis and stream-gradient index. J Res US GeolSurv, 1(4): 421–429

Hanley J T (1977). Fourier analysis of the Catawba Mountain knolls, Roanoke county, Virginia. J Int Assoc Math Geol, 9(2): 159–163

Harrison J M, Lo C P (1996). PC-based two-dimensional discrete Fourier transform programs for terrain analysis. Comput Geosci, 22 (4): 419–424

Horton R E (1945). Erosional development of streams and their drainage basins: hydrophysical approach to quantitative morphology. Geol Soc Am Bull, 56(3): 275–370

Huang N E, Shen Z, Long S R, Wu M C, Shih H H, Zheng Q, Liu H H (1998). The empirical mode decomposition and the Hilbert spectrum for nonlinear and non-stationary time series analysis. In: Proceedings of the Royal Society of London A: Mathematical, Physical and Engineering Sciences, 454(1971): 903–995

Jiang W, Han Z, Zhang J, Jiao Q (2016). Stream profile analysis, tectonic geomorphology and neotectonic activity of the Damxung-Yangbajain rift in the south Tibetan Plateau. Earth Surf Process Landf, 41(10): 1312–1326

Lei A L, Tang K L, Wang W L (2000). Significant and character of conception of soil erosion chain. J Soil Water Conserv, 14(3): 79–83 (in Chinese)

Li F, Tang G, Wang C, Cui L, Zhu R (2016). Slope spectrum variation in a simulated loess watershed. Front Earth Sci, 10(2): 328–339

Li X T, Zhu G X, Cao H Q, Peng F Y (2007). Anisotropy multi-scale self-similarity random field and terrain construction. Journal of Image and Graphics, 12(7): 1286–1290 (in Chinese)

Li Z L (2008). Multi-scale digital terrain modelling and analysis. In: Zhou Q, Lees B, Tang G, eds. Advances in Digital Terrain Analysis. Lecture Notes in Geoinformation and Cartography. Berlin, Heidelberg: Springer, 59–83

Li Z, Zhang Y, Zhu Q, He Y, Yao W (2015). Assessment of bank gully

development and vegetation coverage on the Chinese Loess Plateau. Geomorphology, 228: 462–469

Liu D S, Ding Z, Guo Z (1991). Loess, Environment, and Global Change. Beijing: Science Press

Liu Y B, Zhu X M, Zhou P H (1988). The laws of hillslope channel erosion occurrence and development on loess plateau. Memoir of NISWC Academia Sinica, 7(1): 9–18 (in Chinese)

Luo L X (1956). A tentative classification of landforms in the Loess Plateau. J Geogr Sci, 22(3): 201–222

Ma T, Chen Y, Hua Y, Chen Z, Chen X, Lin C, Yang C (2017). DEM generalization with profile simplification in four directions. Earth Sci Inform, 10(1): 29–39

Perron J T, Kirchner J W, Dietrich W E (2008). Spectral signatures of characteristic spatial scales and nonfractal structure in landscapes. J Geophys Res Earth Surf, 113(F4): F04003

Pike R J, Rozema W J (1975). Spectral analysis of landforms. Ann Assoc Am Geogr, 65(4): 499–516

Rayner J N (1972). The application of harmonic and spectral analysis to the study of terrain. In: Chorley R J, ed. Spatial Analysis in Geomorphology. London: Methuen & Co. Ltd., 283–302

Sun W, Shao Q, Liu J, Zhai J (2014). Assessing the effects of land use and topography on soil erosion on the Loess Plateau in China. Catena, 121: 151–163

Svoray T, Markovitch H (2009). Catchment scale analysis of the effect of topography, tillage direction and unpaved roads on ephemeral gully incision. Earth Surf Process Landf, 34(14): 1970–1984

Tang K, Zhang K, Lei A (1998). Critical slope gradient for compulsory abandonment of farmland on the hilly Loess Plateau. Chin Sci Bull, 43(5): 409–412

Telbisz T, Kovács G, Székely B, Szabó J (2013). Topographic swath profile analysis: a generalization and sensitivity evaluation of a digital terrain analysis tool. Z Geomorphol, 57(4): 485–513

Torri D, Poesen J (2014). A review of topographic threshold conditions for gully head development in different environments. Earth Sci Rev, 130: 73–85

Valentin C, Poesen J, Li Y (2005). Gully erosion: impacts, factors and control. Catena, 63(2–3): 132–153

Vandaele K, Poesen J, Govers G, van Wesemael B (1996). Geomorphic threshold conditions for ephemeral gully incision. Geomorphology, 16(2): 161–173

Wu F (2003). Scale-dependent representations of relief based on wavelet analysis. Geo Spat Inf Sci, 6(1): 66–69

Wu Z, Huang N E (2004). A study of the characteristics of white noise using the empirical mode decomposition method. In: Proceedings of the Royal Society of London A: Mathematical, Physical and Engineering Sciences, 460(2046): 1597–1611

Wu Z, Huang N E (2005). Statistical significance test of intrinsic mode functions. Hilbert–Huang Transform and Its Applications. World Scientific Publishing Co. Pte. Ltd., 107–127

Wu Z, Huang N E (2009). Ensemble empirical mode decomposition: a noise-assisted data analysis method. Adv Adapt Data Anal, 1(1): 1–41

Xu M, Li Q, Wilson G (2016). Degradation of soil physicochemical quality by ephemeral gully erosion on sloping cropland of the hilly Loess Plateau, China. Soil Tillage Res, 155: 9–18

Yu Q, Tian J, Liu J (2004). A NOVEL contour-based 3D terrain matching algorithm using wavelet transform. Pattern Recognit Lett, 25(1): 87–99

Zhang H P, Liu S F, Sun Y P, Chen Y S (2006a). The acquisition of local topographic relief and its application: an SRTM-DEM analysis. Remote Sensing for Land & Resources, 18(1): 31–35 (in Chinses)

Zhang H P, Liu S F, Yang N, Zhang Y Q, Zhang G W (2006b). Geomorphic characteristics of the Minjiang drainage basin (eastern Tibetan Plateau) and its tectonic implications: new insights from a digital elevation model study. Isl Arc, 15(2): 239–250

Zhang L T, Li Z B, Wang H, Xiao J B (2016a). Influence of intra-event-based flood regime on sediment flow behavior from a typical agro-catchment of the Chinese Loess Plateau. J Hydrol (Amst), 538: 71–81

Zhang L T, Li Z B, Wang S S (2016b). Spatial scale effect on sediment dynamics in basin-wide floods within a typical agro-watershed: a case study in the hilly loess region of the Chinese Loess Plateau. Sci Total Environ, 572: 476–486

Zhao G, Mu X, Wen Z, Wang F, Gao P (2013). Soil erosion, conservation, and eco-environment changes in the loess plateau of China. Land Degrad Dev, 24(5): 499–510

Zhao S M, Cheng W M, Zhou C H, Chen X (2009). Analysis on the topographic gradient and geographical meaning of Mt. Konggur, in the northern edge of Qinghai-Tibet Plateau. Journal of Geo-information Sciences, 11(6): 753–758 (in Chinese)

Zhu T X (2012). Gully and tunnel erosion in the hilly Loess Plateau region, China. Geomorphology, 153–154: 144–155

Zhu X M (1956). Classification on the soil erosion in the loess region. Acta Pedologica Sinica, 4(2): 99–115 (in Chinese)

Zou B W, Ma W F, Long Y, Hou S S, Zhang L (2011). Extraction method of swath profile based on ArcGIS and its application in landform analysis. Geography and Geo-Information Science, 27(3): 42–44 (in Chinese)